JBC RESEARCH ARTICLE

Rho and riboswitch-dependent regulations of *mntP* gene expression evade manganese and membrane toxicities

Received for publication, August 29, 2024, and in revised form, October 9, 2024 Published, Papers in Press, November 5, 2024,
https://doi.org/10.1016/j.jbc.2024.107967

Anand Prakash[1,‡], **Arunima Kalita**[1,‡], **Kanika Bhardwaj**[1,2,‡], **Rajesh Kumar Mishra**[1], **Debarghya Ghose**[1], **Gursharan Kaur**[1], **Neha Verma**[1,2], **Bibhusita Pani**[3], **Evgeny Nudler**[3,4], **and Dipak Dutta**[1,2,*]

From the [1]Department of Molecular Biochemistry and Microbiology, CSIR Institute of Microbial Technology, Chandigarh, India; [2]Academy of Scientific and Innovative Research (AcSIR), Ghaziabad, Uttar Pradesh, India; [3]Department of Biochemistry and Molecular Pharmacology, New York University Grossman School of Medicine, New York, New York, USA; [4]Howard Hughes Medical Institute, NYU Langone Health, New York, New York, USA

Reviewed by members of the JBC Editorial Board. Edited by Chris Whitfield

The trace metal ion manganese (Mn) in excess is toxic. Therefore, a small subset of factors tightly maintains its cellular level, among which an efflux protein MntP is the champion. Multiple transcriptional regulators and a manganese-dependent translational riboswitch regulate the MntP expression in *Escherichia coli*. As riboswitches are untranslated RNAs, they are often associated with the Rho-dependent transcription termination in bacteria. Here, performing *in vitro* transcription and *in vivo* reporter assays, we demonstrate that Rho efficiently terminates transcription at the *mntP* riboswitch region. Excess manganese activates the riboswitch, restoring the coupling between transcription and translation to evade Rho-dependent transcription termination partially. RT-PCR and Western blot experiments revealed that the deletion of the riboswitch abolishes Rho-dependent termination and thereby overexpresses MntP. Interestingly, deletion of the riboswitch also renders bacteria sensitive to manganese. This manganese sensitivity is linked with the overexpression of MntP. Further spot assays, confocal microscopy, and flow cytometry experiments revealed that the high level of MntP expression was responsible for slow growth, cell filamentation, and reactive oxygen species (ROS) production. We posit that manganese-dependent transcriptional activation of *mntP* in the absence of Rho-dependent termination leads to excessive MntP expression, a membrane protein, causing membrane protein toxicity. Thus, we show a regulatory role of Rho-dependent termination, which prevents membrane protein toxicity by limiting MntP expression.

Mn is an essential trace nutrient that regulates the functions of handful enzymes by serving as a cofactor or through differential metalation. Mn helps detoxify reactive oxygen species by acting as a cofactor of Mn-dependent superoxide dismutase and ribonucleotide reductase under iron starvation and oxidative stress (1–3). Mn also transiently replaces some enzymes' mononuclear iron cofactor, thereby restoring their functions under oxidative stress (4, 5). However, in excess, Mn inhibits cell growth and promotes cell filamentation by interfering with iron homeostasis in *Escherichia coli* (6, 7). Mn homeostasis in *E. coli* is mainly governed by the MntR transcription regulator. Under Mn shock, Mn-bound MntR represses *mntH* and activates *mntP*, which encodes Mn importer and exporter proteins, respectively (6, 8). MntR also represses *mntS*, which encodes a small peptide, to inhibit the MntP-dependent export of Mn (6, 8). It has been observed that the deletion of *mntP* makes *E. coli* cells highly sensitive to Mn (6–8). Several other mechanisms have also evolved to regulate the MntP levels in *E. coli*. For example, the expression of MntP is also regulated by Fur, a regulator that usually regulates iron homeostasis (6). The 5′-untranslated region (UTR) of the *mntP* forms an Mn-dependent riboswitch to upregulate *mntP* expression in *E. coli* (9, 10). All these reports suggest that the MntP-mediated export of Mn is crucial to handling Mn homeostasis.

The riboswitches usually modulate the expression of downstream genes when they are active in the presence of small metabolites (11, 12). Either they promote the formation of an intrinsic terminator inhibiting the transcription or act at the level of translation initiation, occluding the ribosome binding site (10–14). The *E. coli mntP* riboswitch belongs to the *yybP-ykoY* riboswitch family, which is named after the riboswitch-regulated *yybP* and *ykoY* genes of *Bacillus subtilis*, utilizes Mn as a ligand (10, 14–17). Without Mn, the 229 nucleotides long 5′-UTR of *mntP* maintains a "switched off" conformation of the riboswitch, making RBS inaccessible to the ribosome-mediated translation initiation (10). The presence of Mn stimulates alternate "switch-on" conformation, relieving RBS to interact with the ribosome freely (10). Our recent work has shown that the cellular alkaline pH favors the tight binding of Mn to the riboswitch to activate the latter. Mn activates an intrinsic alkalization circuit, overproducing cellular ammonia to attain this alkaline pH (9).

‡ These authors contributed equally to this work.
* For correspondence: Dipak Dutta, dutta@imtech.res.in.
Present addresses for: Arunima Kalita, Department of Bacteriology, University of Wisconsin-Madison, 1550 Linden Drive Madison, Wisconsin 53706; Rajesh Kumar Mishra, Department of Biological Sciences, Indian Institute of Science Education and Research Mohali, Knowledge City, Sector 81, SAS Nagar 140306, India; Debarghya Ghose, Biotech Desk Pvt. Ltd, 3-5-22/2/A Krishnanagar, Secunderabad 500062, India.

© 2024 THE AUTHORS. Published by Elsevier Inc on behalf of American Society for Biochemistry and Molecular Biology. This is an open access article under the CC BY license (http://creativecommons.org/licenses/by/4.0/).

In contrast to *E. coli*, *B. subtilis*, and many pathogenic Gram-positive firmicutes require comparatively high levels of Mn (18). Manganese is essentially needed for the sporulation of *B. subtilis* (18, 19). To sustain their manganese-centric physiology, these organisms employ a wide range of homeostasis mechanisms. *B. subtilis* MntR mainly represses two different types of Mn uptake operons, one encodes a proton-coupled importer, MntH, and another encodes an ABC transporter (MntABCD) (20). Additionally, MntR activates the expression of MneP and MneS, two cation diffusion facilitator efflux pumps, that export Mn in necessity (21). Unlike *E. coli* MntP, the MneP and MneS exporters are not regulated by any riboswitches. However, the two genes, *yybP* and *ykoY*, which encode membrane proteins of unknown functions in *B. subtilis*, are regulated by Mn-dependent riboswitches (10, 14, 15).

The Rho helicase, a hexameric transcription termination factor, binds and threads the RNA through its central channel in a 5′ to 3′ direction. Once Rho recognizes a paused elongation complex (EC), it dissociates the RNA from the template DNA (22–28). Many auxiliary transcription factors can influence the Rho action. For example, elongation factor NusG binds both EC and Rho and stimulates termination ubiquitously (29–31). Rho function requires RNA sequences named Rho utilization (*rut*) sites, characterized by poorly conserved C-rich sequences with relatively little secondary structure (27, 32–34). Since riboswitches are the sufficiently long untranslated RNA portion of transcripts, they frequently act as platforms for Rho-dependent termination. The Mg^{2+}-sensing *mgtA*-riboswitch in *Salmonella enterica*, FMN-sensing *ribB* and *ribM*-riboswitches in *E. coli* and *Corynebacterium glutamicum*, respectively (35–38), lysine-sensing *lysC*-riboswitch, and thiamin pyrophosphate-sensing *thiB*-, *thiC*- and *thiM*-riboswitches from *E. coli* (39) are some examples where Rho-dependent termination is also reported. Despite thorough mechanistic studies, how the joint actions of riboswitch and a Rho-dependent terminator cater an evolutionary advantage to the bacteria to survive better is not addressed yet. The answer to whether the unhindered overexpression of the riboswitch-associated genes in the absence of Rho-dependent termination is detrimental to bacteria is missing.

In the present study, we show that apart from forming a Mn-dependent riboswitch, the 5′-UTR of *mntP* also serves as a platform for the Rho-dependent transcription termination to downregulate *mntP* expression. Mn exposure activated the riboswitch and sufficiently upregulated *mntP* expression by partially suppressing Rho-dependent termination to mitigate Mn stress. The Mn stress overexpressed MntP at a very high level in an *E. coli* strain devoid of the 5′-UTR. The cells exhibited slow growth, ROS production, and filamentation phenotypes. As these phenotypes fit perfectly with the context of membrane protein overexpression, we propose that Rho-dependent termination at the 5′-UTR presumably ensures standard membrane biology by suppressing the uncontrolled expression of MntP membrane protein.

Results

Inhibition of Rho function causes upregulation of mntP *expression*

Due to the presence of a sufficiently long 5′-UTR, we asked whether *mntP* gene expression is suppressed by transcription termination factor Rho. To test this possibility, we treated the growing *E. coli* wild-type (WT) cells with 100 μg/ml of bicyclomycin (BCM), a specific and potent antibiotic against Rho function (31, 40), and isolated the total cellular RNA. Using RT-PCR assay with the oligonucleotides specific for the open reading frame (ORF) of *mntP*, we found that BCM treatment upregulated the *mntP* gene by 20-fold (Fig. 1*A*). This observation suggests that the inactivation of Rho by BCM might block Rho-dependent termination at the 5′-UTR of *mntP*, causing an increased transcriptional read-through in the *mntP* ORF.

Rho-dependent termination at the mntP *gene locus demonstrated by* in vitro *transcription assays*

In order to check whether the BCM-induced increase in *mntP* transcript is a direct result of Rho action, we made an *in vitro* transcription template (T1) fusing T7A1 promoter, which is an *E. coli* RNA polymerase-specific promoter, with 5′-UTR and 147 bp of *mntP* ORF by an overlapping PCR (Fig. 1*B*). A single round *in vitro* transcription assay was performed in the presence or absence of Rho. The transcription products were resolved by a urea-denaturing polyacrylamide gel electrophoresis (Urea-PAGE). Without Rho, the EC generated the full-length transcription run-off (RO) RNA at the end of templates. Some RNA transcripts shorter than the RO product were also generated, as the EC has an inherent tendency to pause at multiple locations during the transcription elongation process (Fig. 1*C*, lane 1). In the presence of Rho, the band intensity of the RO product declined (Fig. 1*C*, lane 2), but the intensity of the shorter RNA bands (Fig. 1*C*, lane 3), corresponding to some of the RNA polymerase pause bands (41) (Fig. 1*C*, lanes 1), were simultaneously increased. NusG is an additional transcription factor that assists the Rho-dependent termination process (29–31). We found that NusG enhanced the intensity of the shorter RNA bands in the presence of Rho (Fig. 1*C*, lane 4).

Although the intense bands of shorter transcripts that appeared in the presence of Rho are usually considered the putative Rho-dependent transcription termination products, they could be the mixture of the actual products of termination and transcriptional pausing of ECs (Fig. 1*D*). To separate the paused and terminated transcripts, we performed transcription assays, immobilizing the biotinylated template on streptavidin beads. The reaction products were separated into pellet and supernatant fractions. In the absence of Rho, most of the transcripts appeared in the pellet, while barely any transcripts were visible in the supernatant fraction in a urea-PAGE (Fig. 1*D*, lanes 4 and 6). However, when Rho was present, most of the shorter transcripts appeared in the

ASBMB

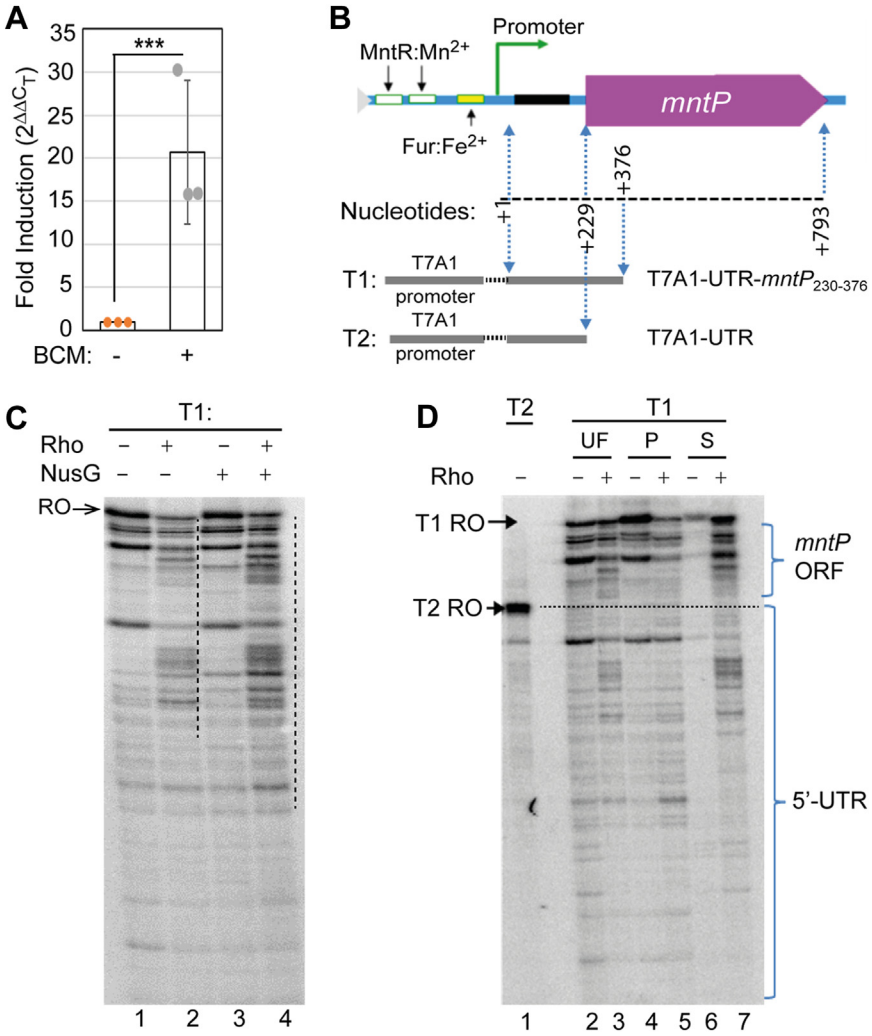

Figure 1. Rho-dependent termination at the *mntP* gene locus. *A*, expression profile of *mntP* gene detected by Rt-PCR experiment. 100 µg/ml of BCM was used. The mean ± s.d. values from three independent experiments were plotted. ***$p < 0.001$, unpaired *t* test. *B*, schematic showing the DNA region at the 5´-UTR, *mntP* ORF, and T7A1 promoter to make T1 and T2 templates. *C*, Phosphor-imaging of 6% urea PAGE showing the *in vitro* transcription products on the T1 template in the presence or absence of Rho and NusG. RO marks the run-off product. The vertical *dotted lines* show the zone of Rho-dependent termination. *D*, phosphor-imaging of 6% urea PAGE shows unfractionated (UF), and fractionated samples (streptavidin pellet (P) and supernatant (S) fractions). The level of RO product using a shorter T2 template is shown.

supernatant than in the pellet fraction (Fig. 1*D*, lanes five and 7). The appearance of transcripts in the supernatant fraction indicates that Rho successfully terminated many transcripts before maturation. A shorter transcriptional RO product using a shorter DNA template, T7A1-UTR (T2), was generated as a marker (Fig. 1, *B* and *D*). The Rho-dependent transcription termination bands that were resolved below or above the position of the T2 RNA marker represent the termination that occurred in the 5′-UTR or initial 147 bp of *mntP* ORF, respectively (Fig. 1*D*). This data elucidates that Rho may terminate transcription at the 5′-UTR as well as at the ORF region of *mntP*.

The activated riboswitch partially overcomes Rho-dependent termination

We then asked how the Rho-dependent termination affects the *mntP* riboswitch function or *vice versa*. The Mn activates the MntR regulator at the *mntP* promoter or *mntP*-riboswitch (6, 10). Therefore, to specifically check the riboswitch activation, we replaced the native promoter with the T7A1 constitutive promoter, which would not be regulated by Mn, to design three reporter strain constructs (construct 1, construct 2, and construct 3) (Fig. 2*A*). T7A1 promoter followed by the 5′-UTR and a portion of *mntP* ORF (encompasses +1 to +439 bp) was transcriptionally fused with either *lacZ* or YFP reporters. The reporter cassettes were integrated into the *E. coli* WT chromosome to generate the construct 1 and 2 reporter strains of *E. coli* (Fig. 2*A*). The design of the construct three will be described in a later section. Consistent with the RT-PCR trend (Fig. 1*A*), BCM treatment (100 µg/ml) enhanced the β-galactosidase activity and YFP fluorescence up to about 23 and 28-folds, in the construct one and 2, respectively (Fig. 2, *B* and *C*). This observation suggests that *in vivo* Rho-dependent termination at the *mntP* locus suppresses reporter expressions.

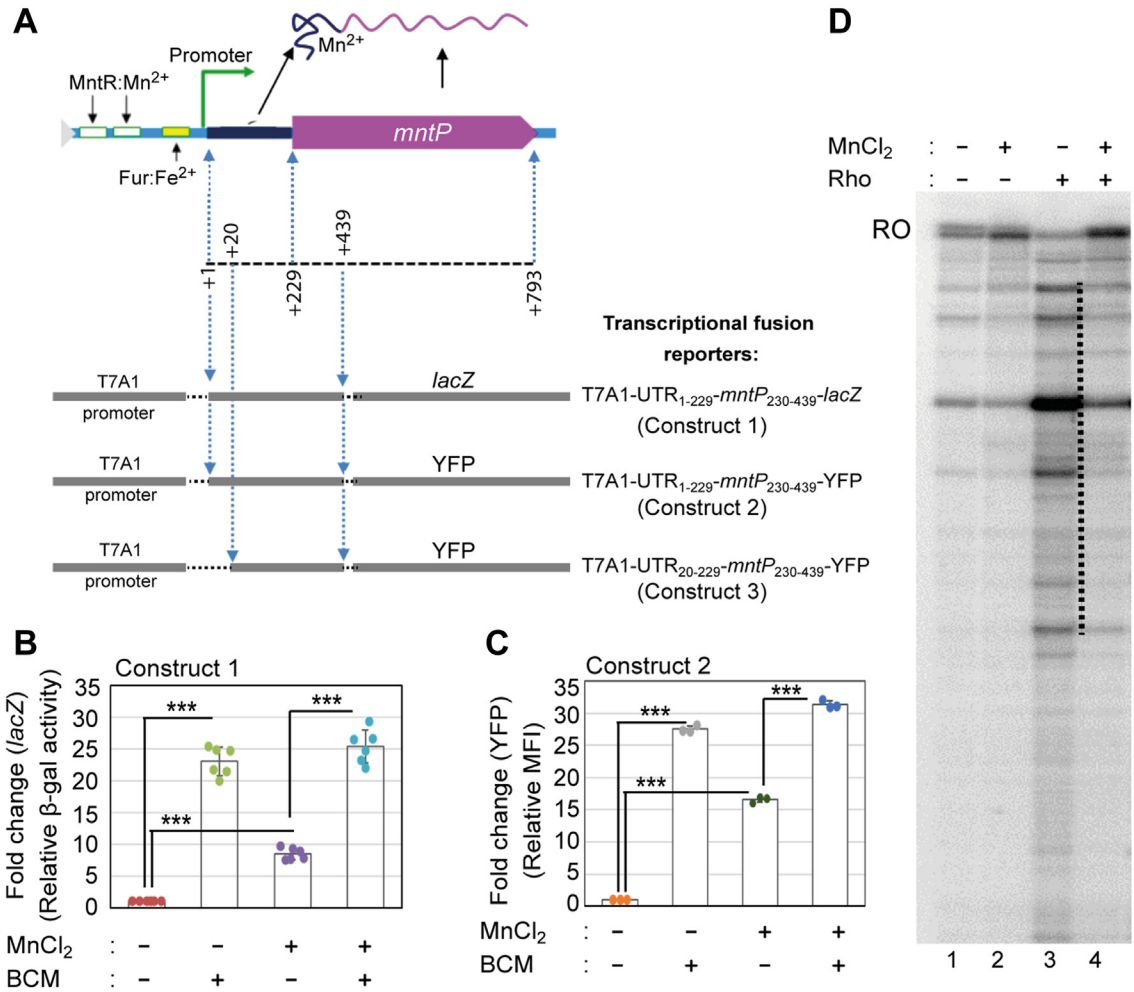

Figure 2. The reporter assays to demonstrate that Rho prematurely terminates *mntP* expression. *A*, the schematic shows the DNA fragments from the 5′-UTR and *mntP* ORF that have been fused with T7A1 promoter and YFP or lacZ reporters to make the reporter cassettes. *B*, the β-galactosidase activity from construct one in the presence or absence of 100 μg/ml BCM and 8 mM Mn are plotted. The calculated Miller unit for construct one was 545.5 ± 41. The values are mean ± s.d. from six independent experiments. ***$p < 0.001$, unpaired *t* test. *C*, the estimated MFI of YFP from construct two are exhibited. The calculated values are mean ± s.d. from three independent experiments. ***$p < 0.001$, unpaired *t* test. *D*, phosphor-imaging of *in vitro* transcription products on the T1 template in the presence or absence of Rho, and/or 100 μM Mn.

We also tested the effect of Mn on the expression profile of reporter constructs one and two. The $MnCl_2$ (8 mM) shock (since 8 mM exogenous Mn causes sufficient toxicity in *E. coli* WT cells (18)) enhanced both β-galactosidase activity (9-folds) and YFP fluorescence (16-folds) (Fig. 2, *B* and *C*). BCM treatment to the Mn-fed *E. coli* cells further enhanced the β-galactosidase activity (25-folds) and YFP fluorescence (30-folds) that are comparable to the levels achieved by BCM treatment alone (Fig. 2, *B* and *C*). This observation indicates that while the Mn-mediated riboswitch activation partially upregulates the reporters, most of the transcripts still remain under regulation by Rho-dependent termination. In other words, Mn could partially inhibit Rho-dependent termination by activating *mntP* riboswitch to upregulate the reporter genes.

To address whether Mn directly interacts with Rho, thereby affecting Rho-dependent termination at the *mntP* riboswitch, we performed an *in vitro* transcription assay on the T1 template to test termination in a clean system. In the presence of Mn, longer transcripts representing transcription runoff re-appeared in a reaction containing termination factor Rho (Fig. 2*D*). However, unlike *in vivo* assay, here we detected a complete inhibition of Rho-dependent termination, possibly due to constraints in creating an identical *in vivo* situation in an *in vitro* assay. Nevertheless, the results, mainly the *in vivo* observation, support that *mntP* 5′-UTR serves as an Mn-dependent riboswitch by dialing down Rho-dependent termination.

Free Mn does not influence Rho's function

To test whether free Mn directly affects Rho's termination function, we performed the following experiments. From the predicted structure of *mntP* riboswitch (10), we assumed that the absence of +1 to +19 nucleotides of the 5′-UTR would diminish the riboswitch activation while allowing the synthesis of a sufficiently long untranslated RNA for Rho-dependent termination. To test this possibility, we designed the third reporter strain (construct 3), where the T7A1 promoter

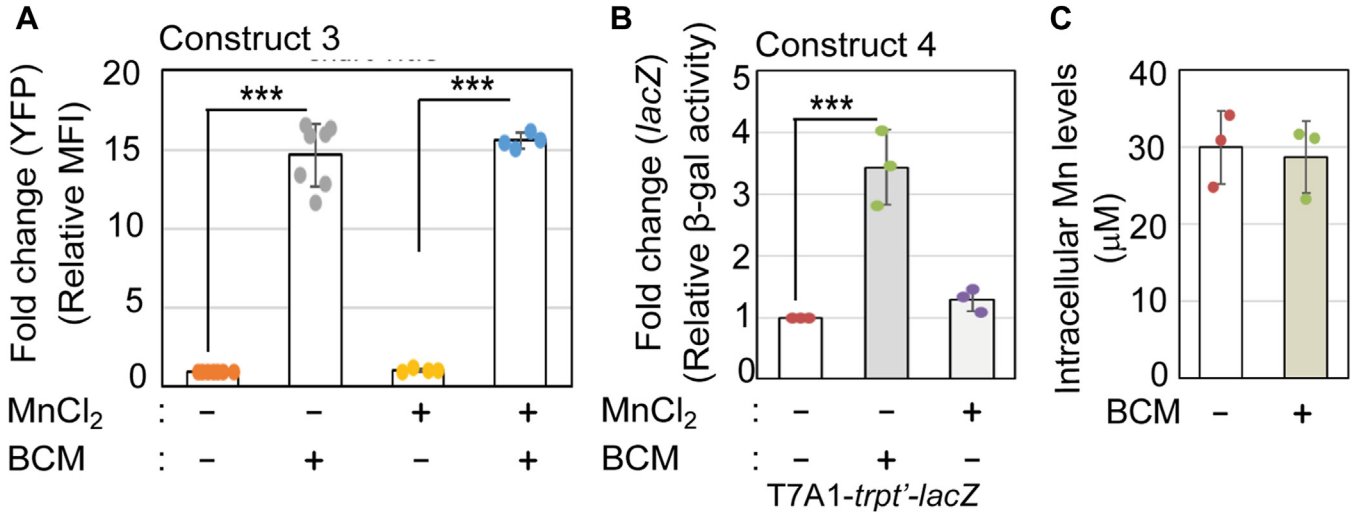

Figure 3. Free Mn and Rho do not affect each other's actions. *A*, the YFP fluorescence (MFI) values in construct three are plotted. 8 mM Mn or 100 μg/ml BCM were used, as indicated. The values are mean ± s.d. values from six independent experiments. ***$p < 0.001$, unpaired *t* test. *B*, the relative β-galactosidase activities in construct four containing *trp t'* terminator are plotted. 8 mM Mn or 100 μg/ml BCM were used, as indicated. The calculated Miller unit for constructing four without any treatment was 4428 ± 902. The values are mean ± s.d. from three independent experiments. ***$p < 0.001$, unpaired *t* test. *C*, the cellular Mn level in the presence or absence of 100 μg/ml BCM are plotted. The calculated mean ± s.d. values from three independent experiments were plotted. ***$p < 0.001$, unpaired *t* test.

followed by +20 to +439 bases of the *mntP* gene was fused with a YFP reporter and integrated into the WT strain (Fig. 2*A*). Indeed, Mn at 8 mM did not affect the mean fluorescence intensity (MFI) of YFP in construct 3 (Fig. 3*A*), suggesting that the absence of initial 19 residues in the 5′-UTR impair the formation of the Mn riboswitch. On the other hand, BCM alone, or BCM treatment to the Mn-fed construct three strain, increased the MFI of YFP to 15-fold (Fig. 2*D*). This observation indicates that the free Mn that could not form a complex with the truncated riboswitch has no effect on Rho function, and BCM-mediated inactivation of Rho directly allows transcription through the 5′-UTR to express YFP reporter.

To further ensure that Mn has no direct influence on the Rho function, we made another construct (construct 4), where the T7A1 promoter was fused with *trp t'* DNA that encodes a well-known Rho-termination site (24, 28, 42), and followed by a *lacZ* reporter. Using this construct, we show that 8 mM Mn did not affect the Rho-dependent termination process (Fig. 3*B*). Besides performing ICP-MS analyses, we determined that inactivating the Rho-dependent termination by BCM did not increase the cellular Mn levels (Fig. 3*C*). All these results suggest that Mn shock and Rho-dependent termination do not directly influence each other in affecting cellular physiology.

E. coli *is Mn-sensitive in the absence of the 5′-UTR*

We deleted the riboswitch (except +1 to +20 bp region) from the WT strain to get the riboswitch-deleted strains (Δ*RS*::*kan*^{R} and Δ*RS* strains) by the λ-red recombination system (43). Thus, we expected that the absence of 5′-UTR would defy Rho-dependent termination at the upstream of the *mntP* gene. This situation would lead to upregulation of MntP, causing a manganese-resistant phenotype in the riboswitch-deleted strains. To our surprise, the riboswitch-deleted strains unexpectedly exhibited Mn-sensitivity when grown on an LB-agar plate supplemented with 2 mM $MnCl_2$ (Fig. 4*A*). The *E. coli* Δ*mntP* strain that fails to eject out excess Mn is also highly Mn-sensitive (7). Performing growth curve analyses, we find that 1 mM and 3 mM Mn caused roughly equivalent extents of growth defects to the Δ*mntP* and the Δ*RS* strains, respectively (Fig. 4*B*).

Performing confocal microscopy, we checked cellular morphology in the presence or absence of Mn. The WT strain exhibited a typical average cell length (2.22 ± 0.54 μM). In comparison, the Δ*RS* strain showed a significant increase in average cell length (3.47 ± 1.47 μM) in LB broth (Figs. 4*C* and S1). Under 2 mM Mn shock, the WT strain showed a significant but minor increase in average cell length (2.62 ± 0.81 μM), while the Δ*RS* strain was filamented (10.1 ± 3.95 μM) (Figs. 4*C* and S1). The filamentous phenotype of ΔRS strain was further analyzed by FM-4-64 and DAPI staining to show that the nucleoids were segregated but there was no septum formation in the filamentation (Fig. S2). Interestingly, the Δ*mntP* strain also exhibits Mn-dependent cell filamentation (7). In summary, the absence of *mntP* (in the Δ*mntP* strain) and the absence of the Rho-dependent termination/riboswitch function in the riboswitch-deleted strains both caused growth retardation and inhibition of cell division under Mn shock.

The absence of the 5′-UTR overexpresses MntP under manganese stress

The above observations raised a question of whether the Δ*RS* strain fails to express *mntP* and thereby mimics Δ*mntP*-like phenotypes. However, we noticed quite the opposite results when checking the expression of MntP by RT-PCR

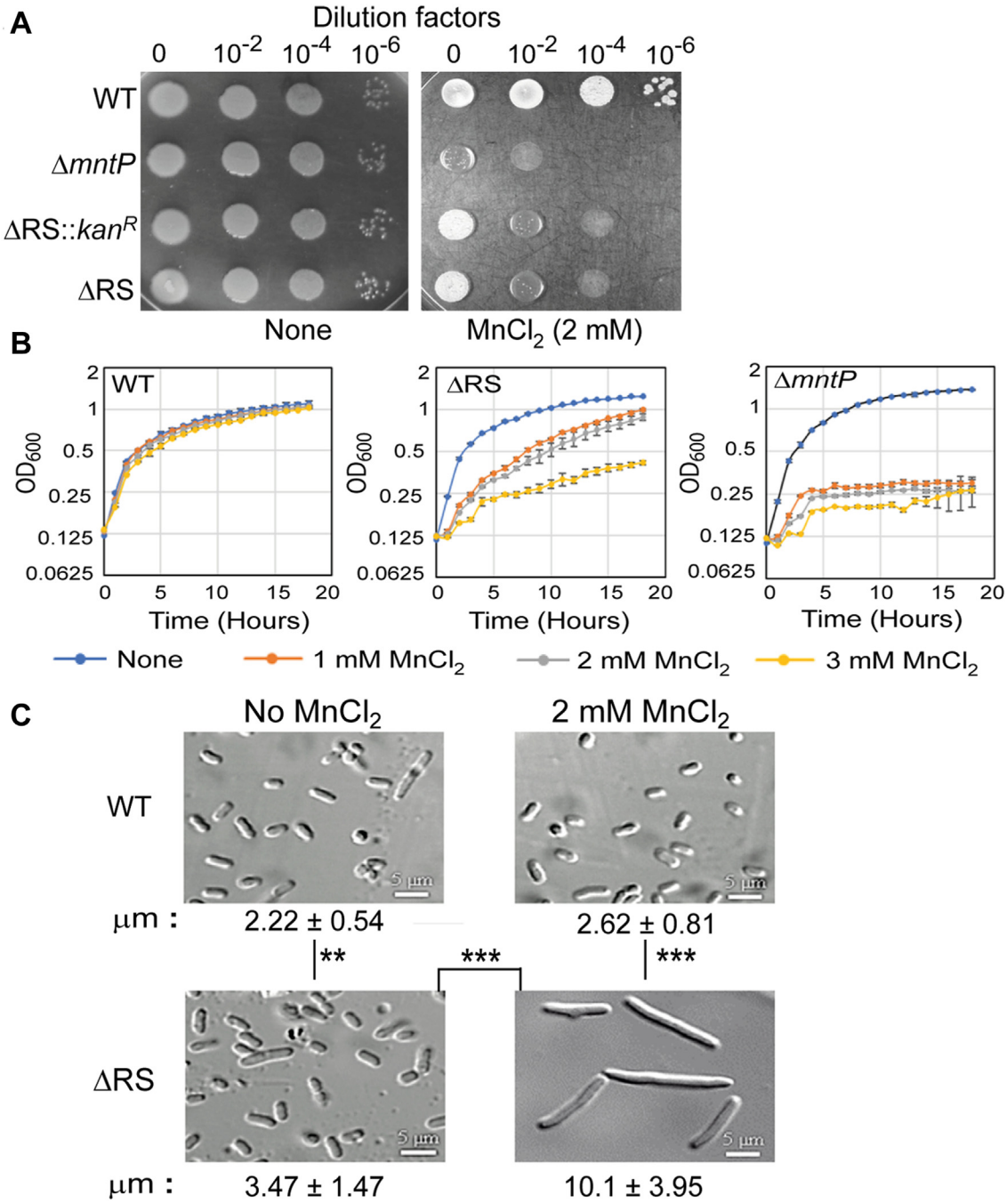

Figure 4. Rho-dependent termination at 5′-UTR inhibits membrane protein toxicity. *A*, the spot assay shows that the riboswitch-deleted strains (Δ*RS::kan*^{R} and Δ*RS*) are Mn-sensitive. *B*, the WT, ΔRS, and Δ*mntP* strains were grown in the absence or the presence of different concentrations of Mn to compare the Mn sensitivity. *C*, confocal microscopy images show the cell filamentation of different strains of *E. coli*. The μM length of cells was calculated (mean ± s.d. values from 30-50 cells) and shown. $^{**}p < 0.01$; $^{***}p < 0.001$, unpaired *t* test. Fig. S1 exhibits a bigger area covering a greater number of cells.

experiments. Mn at 1 mM, which is nontoxic to the WT cells (Fig. 4*A*), slightly enhanced the expression of *mntP* (2.5-folds) (Fig. 5*A*). When treated with a toxic dose (8 mM) of Mn (9), the WT cells exhibited about 11-fold upregulation of *mntP* (Fig. 5*A*). The Δ*RS* strain showed an inherently high level of *mntP* expression (7-folds) even in the absence of Mn shock (Fig. 5*A*). Strikingly, Mn at 1 mM and 2 mM levels increased this expression to about 19 and 70-fold, respectively (Fig. 5*A*). We assume that the activation of the MntR regulator by Mn upregulated the *mntP* in the Δ*RS* strain. Consistent with this assumption, unlike Δ*RS strain*, the Δ*mntR* Δ*RS* strain failed to upregulate *mntP* in the presence of 2 mM $MnCl_2$ (Fig. 5*A*).

We also checked the cellular MntP protein level performing western blotting experiments. For this, we engineered the chromosome of WT and Δ*RS* strains by incorporating 3X-FLAG epitope-tag-coding sequence at the C-terminal end of *mntP* ORF. Using anti-FLAG antibody, we show that the

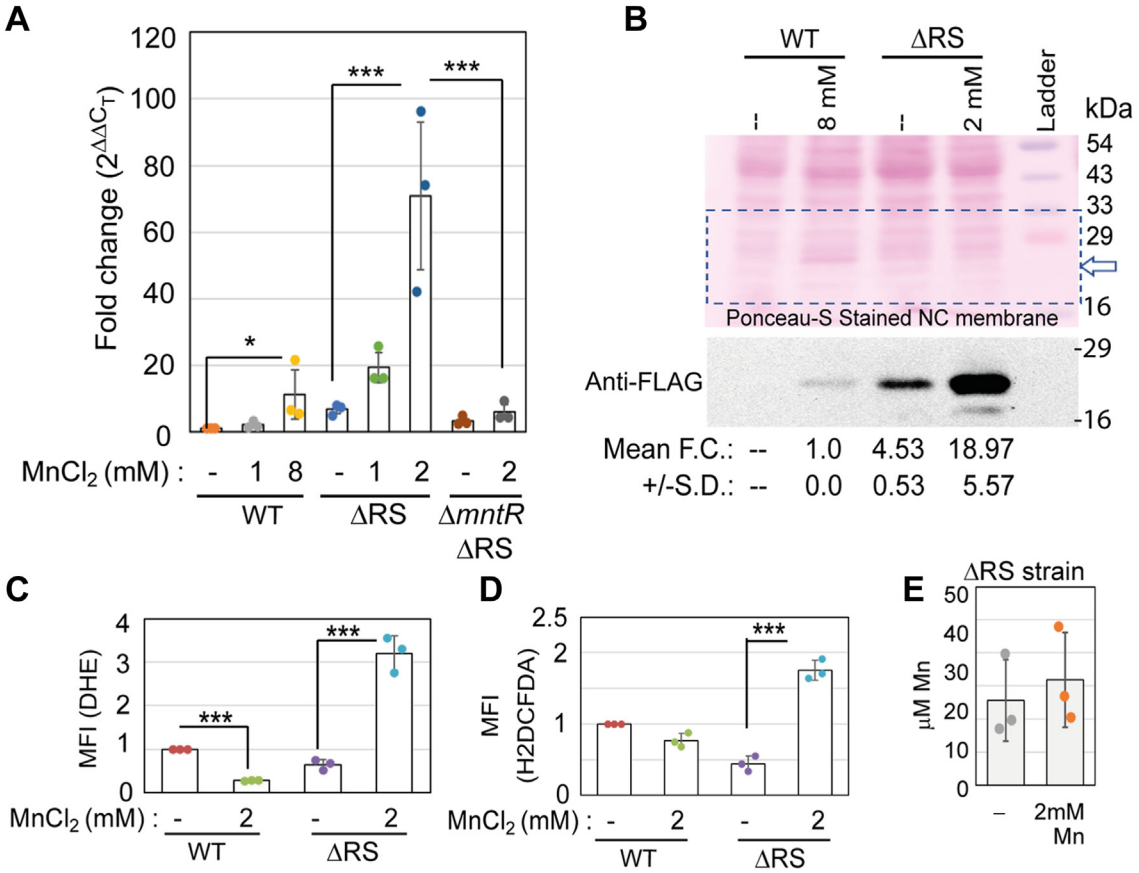

Figure 5. Mn excessively upregulates *mntP* in the ΔRS strain. *A*, RT-PCR data show the *mntP* gene expression in the WT, Δ*RS*, and Δ*mntR* Δ*RS* strains in the presence or absence of Mn. The values are mean ± s.d. from three independent experiments. *$p < 0.1$; **$p < 0.01$, unpaired *t* test. *B*, Western blotting experiment shows overexpression of MntP-FLAG in the presence of Mn. The anti-FLAG signal remained below the detection level for untreated WT cells in our assay. Fold change (F.C.) values (mean ± s.d) were calculated using Image J software from three different Anti-FLAG blots and normalized against Mn-fed WT samples. Ponceau-S-stained membrane is shown to visualize the equal loading of the cellular proteins. *C*, the ROS-detecting probe, DHE, was used to show the fluorescence (MFI) from the WT and Δ*RS* strains in the presence or absence of Mn. The values are mean ± s.d. from three independent experiments. ***$p < 0.001$, unpaired *t* test. *D*, the ROS detecting probe, H2DCFDA, was used to fluorescence (MFI) from the WT and Δ*RS* strain in the presence or absence of Mn. The values are mean ± s.d. from three independent experiments. ***$p < 0.001$, unpaired *t* test. *E*, ICP MS analysis to check the intracellular levels of Mn (mean ± S.D) in the unfed and Mn-fed Δ*RS* strain.

exposure to the 8 mM Mn upregulated MntP in the WT strain compared to the untreated control (Fig. 5*B*). The Δ*RS* strain naturally exhibited a high basal level of MntP expression, suggesting that the absence of the Rho-dependent termination upregulated the MntP protein (Fig. 5*B*). The MntP level was excessively increased upon 2 mM Mn shock in the Δ*RS* strain (Fig. 5*B*).

The upregulation of *mntP* in the Mn-treated Δ*RS* strain was found to be associated with oxidative stress, as observed using dihydroethidium (DHE) and 2′,7′-dichlorodihydrofluorescein diacetate (H2DCFDA), two different ROS detecting chemicals (Fig. 5, *C* and *D*). This data is consistent with a previous observation that has shown that the *mntP* overexpression from a plasmid leads to oxidative stress in *E. coli* (44). Furthermore, we estimated the metal content of the cells to show that the Δ*RS* strain exhibited 25.6 ± 12 μM and 31.9 ± 14 μM intracellular Mn, respectively, in the absence or presence of 2 mM extracellular Mn, suggesting that MntP overexpression in the Mn-fed Δ*RS* strain did not deplete the cellular Mn levels (Fig. 5*E*).

The overexpression of MntP in the ΔRS strain appears to be toxic

We observed growth defects and cell filamentation of the ΔRS strain under Mn shock (Fig. 4) despite the overexpression of MntP protein (Fig. 5). Therefore, we hypothesize that the Mn-sensitivity of the ΔRS strain may be the result of an excessive overexpression of MntP under Mn shock. To directly check whether *mntP* overexpression is toxic, we transformed the Mn-sensitive Δ*mntP* strain with an arabinose inducible pBAD-*mntP* expression vector. The multicopy leaky expression of *mntP* from the plasmid sufficiently rescued the Mn-sensitive growth phenotype of the Δ*mntP* strain (Fig. 6*A*). As a control, the Δ*mntP* strain harboring the pBAD empty vector did not rescue the Mn-dependent growth inhibition (Fig. 6*A*). However, when *mntP* expression from the pBAD-*mntP* vector was induced by 0.002% arabinose, the Δ*mntP* strain showed extreme growth retardation (Fig. 6*A*). Similar to the Mn-fed Δ*RS* strain (Fig. 4*C*), the overexpression of *mntP* from the plasmid led to cell filamentation (Figs. 6*B* and S3).

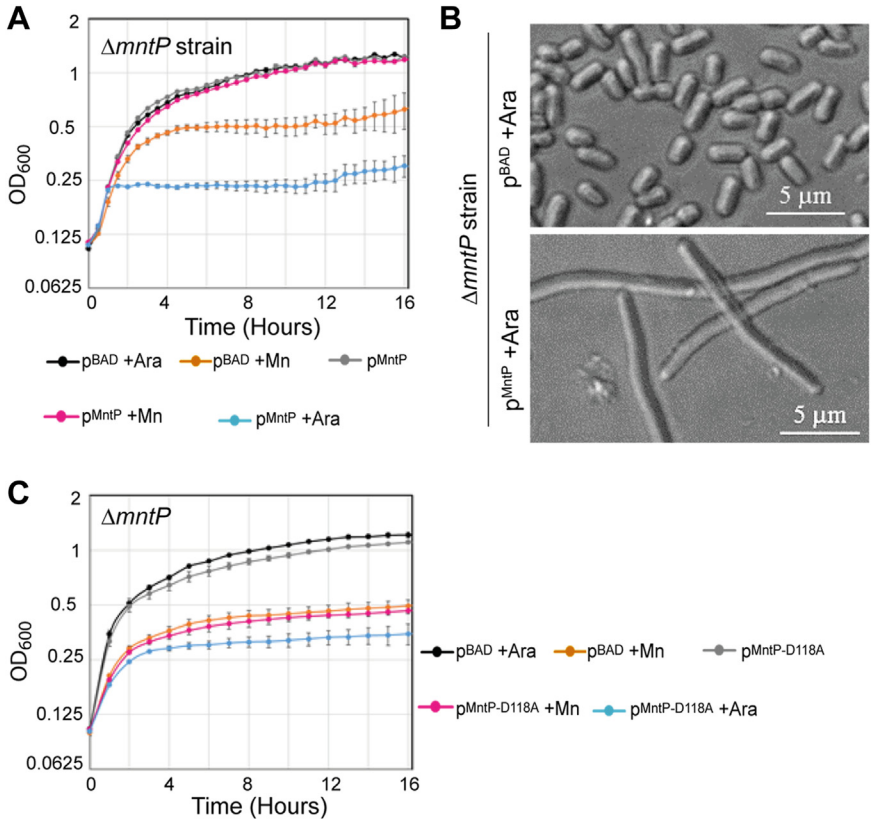

Figure 6. Multicopy overexpression of MntP from an overexpressing plasmid is toxic. *A*, the growth curves show the growth effect when multicopy induction of MntP by arabinose (0.002%) was done in the Δ*mntP* strain. The calculated mean ± s.d. values from three independent experiments were plotted. *B*, the multicopy induction of MntP leads to cell filamentation. Fig. S3 shows bigger fields covering a greater number of cells. *C*, the growth curves assess the effect of multicopy induction of $MntP^{D118A}$, which is a nonfunctional MntP, by arabinose (0.002%) in the Δ*mntP* cells. The calculated mean ± s.d. values from three independent experiments were plotted.

One may argue that an excessive Mn export by overexpressed MntP may lead to growth inhibition phenotype. To test this, we used a nonfunctional MntP mutant ($pMntP^{D118A}$ transformed in the Δ*mntP* strain) (44) in the growth assay. The multicopy induction of $MntP^{D118A}$ by arabinose (0.002%) did not rescue the growth defect (Fig. 6*C*). These data suggest that MntP overexpression but not its function is toxic to the cells.

MntR-mediated transcriptional activation does not suppress Rho-dependent termination

We grew *E. coli* WT cells in the presence or absence of Mn and BCM to check whether MntR-mediated transcriptional upregulation can suppress Rho-dependent termination. Performing RT-PCR, we observed that $MnCl_2$ and BCM separately upregulate *mntP* to about 15 and 30-folds (Fig. 7*A*). When the growing cells were treated with both $MnCl_2$ and BCM together, a further increase in *mntP* expression (120-folds) was observed (Fig. 7*A*). We also performed western blotting experiments to show that Mn and BCM separately upregulated the MntP-FLAG expression, but the expression was highest when the growing cells were treated with $MnCl_2$ and BCM together (Fig. 7*B*). These experiments suggest that *mntP* upregulation by MntR under Mn stress increases the level of *mntP* but this process does not influence the Rho-dependent termination. MntR and Rho act at two distinct phases of transcription, *viz.*, at the transcription initiation and elongation phases, respectively. The sites of their action are also spatially separated, *viz.*, MntP binds at the promoter DNA element, while Rho binds at the sufficiently long nascent mRNA to initiate a termination. Moreover, Rho is an abundant protein that remains in almost equimolar level that of RNA polymerase EC in the *E. coli* cells (27). Given these facts, it is quite possible that the Rho could catch up and terminate *mntP* transcripts at the elongation phase even when MntR upregulated the *mntP* gene at the initiation phase.

Discussion

Our current study demonstrates that Rho is pivotal in terminating the transcription of *mntP* at the riboswitch. In the presence of Mn stress, the active form of the Mn^{2+}:*mntP*-riboswitch switches on the translation (10), thereby partially evading Rho-dependent transcription termination and allowing MntP expression (Fig. 2, *B* and *C*). Thus, efflux of Mn by overexpressed MntP mitigates manganese stress.

A tight coupling between transcription and translation processes, *in vivo*, usually evades the Rho-mediated termination at the ORF (45, 46). In the absence of Mn, riboswitch's "switched off" conformation masks the SD site (10), and thereby the former would uncouple the transcription and

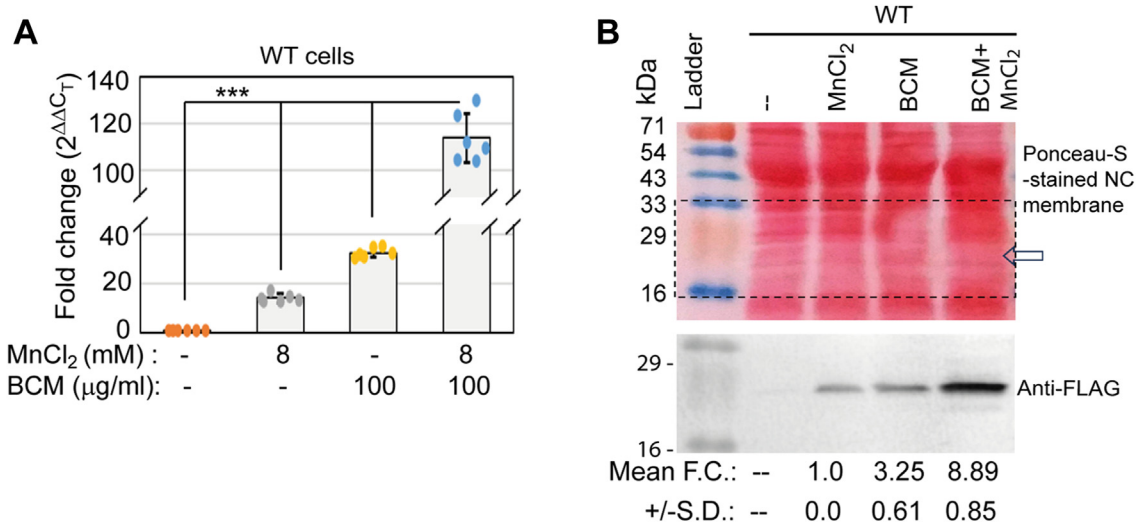

Figure 7. MntR-mediated upregulation of *mntP* does not impact the Rho-dependent termination. *A*, the expression levels of *mntP* observed in the presence or absence of Mn (8 mM), BCM (100 μg/ml) or both. The fold change values (mean ± s.d.) from three independent experiments were plotted. ***$p < 0.001$, unpaired *t* test. *B*, the Western blot experiments show the effect of Mn (8 mM), BCM (100 μg/ml) or both on MntP-FLAG expression. The anti-FLAG band intensities were calculated by Image J software. The band intensities were normalized and plotted. The anti-FLAG band remained below detection level in the untreated sample. The fold change values (mean ± s.d.) are from three independent blots.

translation processes. Thus, Rho-dependent termination suppresses roughly 24/25th parts of the reporter gene expression, while only 1/25th of parts could be expressed under the conditions examined (Fig. 2, *B* and *C*). In the presence of Mn shock, the alternative "switch on" conformation of riboswitch would evade Rho-dependent transcription termination in two different ways: one is by directly inhibiting Rho-binding to the RNA, and the other is by unmasking the SD, thereby facilitating transcription and translation coupling. Thus, under Mn stress, a modest increase (about 8/25th parts) in β-galactosidase activity was observed (Fig. 2, *B* and *C*).

While most riboswitches from *B. subtilis* affect intrinsic termination (11, 47), the *E. coli* riboswitches work primarily by modulating translation initiation (48). Consistently, the *mntP* riboswitch of *E. coli* works at the level of translation initiation (10). Interestingly, the majority of the *E. coli* riboswitches employ Rho-dependent transcription termination (35, 39). Rho is abundant and essential in *E. coli*; therefore, the scope of Rho-dependent termination is widespread in *E. coli* (27, 31, 49). On the other hand, Rho is scarce and dispensable in *B. subtilis*; therefore, most of the terminators are intrinsic in *B. subtilis* (50, 51). Accordingly, the binding of Mn to *yybP-ykoY* riboswitch precludes termination at the intrinsic terminator in upstream of *yybP* and in the leader region of *ykoY* (15). In *Lactococcus lactis*, another Gram-positive bacterium, a similar intrinsic terminator formation at the *yybP-ykoY* riboswitch region has been proposed at low Mn level (14). Thus, generalizing others' (35, 39) and our current observations, it appears that the active riboswitches in *E. coli* defy the Rho-dependent termination by coupling transcription and translation processes and thereby allow gene expression. Whether this generalization has a broader scope for Gram-negative and Gram-positive bacteria needs to be deciphered.

Despite the riboswitch suppressing Rho-dependent termination, the bulk of total transcription (about 17/25th parts) was still prematurely terminated by Rho under the conditions examined (Fig. 2, *B* and *C*). We argued that most of the time, Rho quickly gets access to the nascent free RNA as it migrates with the EC (28) before Mn could form a complex with RNA to "switch on" the riboswitch under *in vivo* conditions. This argument explains how Rho-dependent termination at the *mntP*-riboswitch region ensures a substantially low level of MntP expression both in the presence or absence of Mn stress.

We demonstrate that when Rho-dependent termination at the riboswitch RNA was defied in the Δ*RS* strain, an inherently high level of *mntP* expression was detected (Fig. 5, *A* and *B*). Mn stress increased this expression further (Fig. 5, *A* and *B*). However, why does Rho ensure low-level expression of MntP? We hypothesize that since MntP is an inner membrane protein, the Rho-dependent termination could suppress its expression to evade membrane protein toxicity. Generally, the overexpression of inner membrane proteins is highly toxic and leads to growth defects and cell filamentation (52–55), as we also observed the same phenotype when MntP is overexpressed (Figs. 4 and 6). Therefore, we propose that the Rho-dependent transcription termination acts to suppress membrane protein toxicity by silencing MntP expression under Mn stress, as shown in the schematic (Fig. 8).

The mechanism of cytoplasmic membrane protein toxicity may be multifold. The membrane protein overexpression may exhaust the limited membrane space, leaving little room for others to be integrated, or may affect enzyme functions, especially those involved in oxidative phosphorylation/ATP synthesis (52, 53, 55). Besides, such overexpression may inhibit some crucial cellular functions by nonspecific electrostatic interaction with other membrane proteins (56). From our

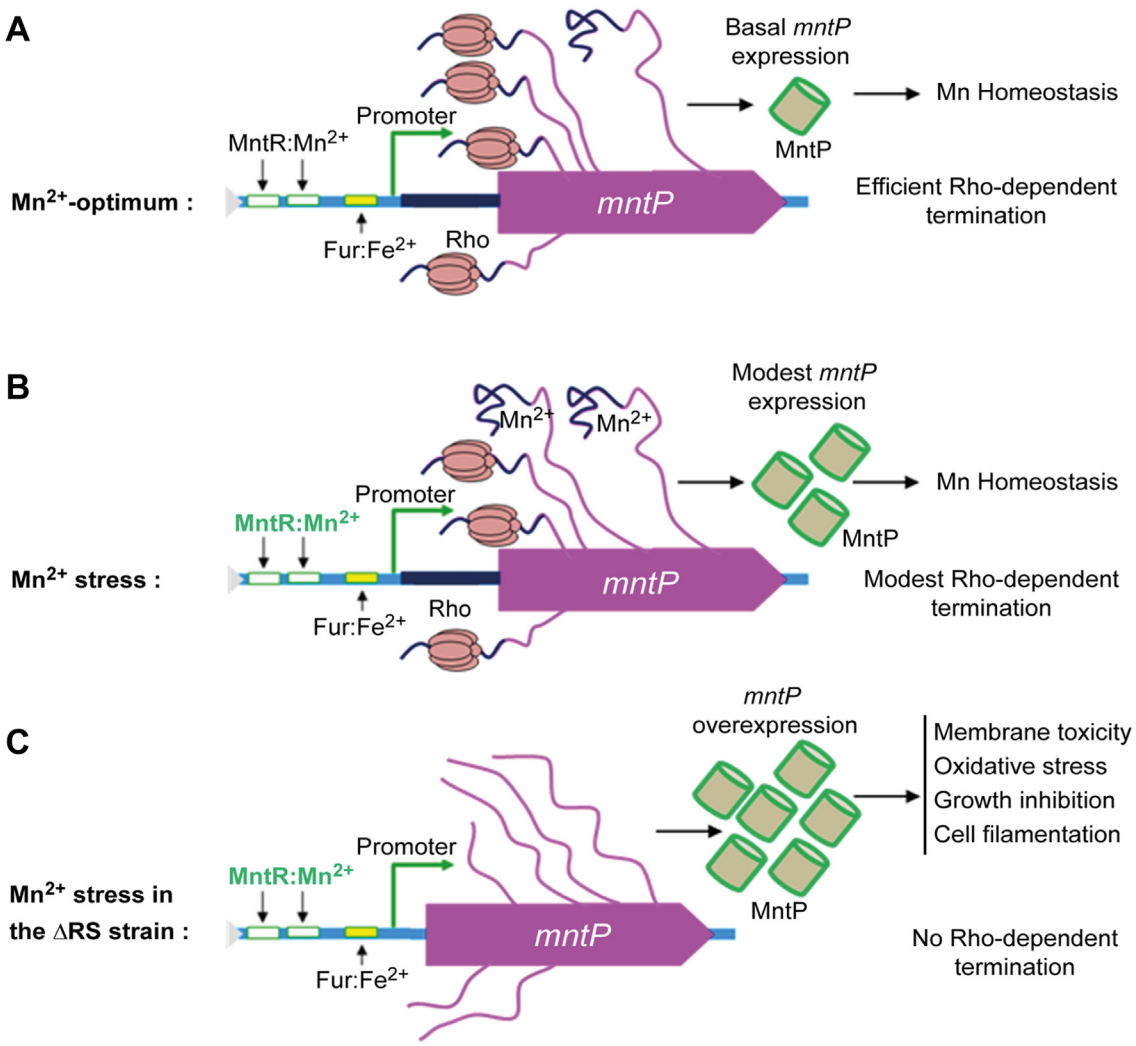

Figure 8. Schematic showing the regulation of *mntP* expression by Rho and Mn. *A*, at optimum cellular Mn, Rho prematurely terminates transcripts at the *mntP* locus. Besides, MntR and riboswitch-mediated regulations also remain silent. All these aspects ensure a basal level of *mntP* expression for Mn homeostasis. *B*, under Mn stress, the active MntR: Mn^{2+} regulator, and the activated riboswitch, upregulate MntP to some extent. However, the majority of transcripts are still terminated by Rho prematurely, causing the modest level of MntP expression. *C*, in the case of the ΔRS strain, the absence of riboswitch RNA evades the Rho-dependent termination. Mn stress further activated the MntR regulator to upregulate MntP. Therefore, MntP was overexpressed uncontrollably, causing membrane protein toxicity.

study, it appears that MntP overexpression possibly perturbed membrane biology and produced ROS, causing the slow growth and cell filamentation phenotypes (Figs. 4 and 6).

Experimental procedures

Bacterial strains, growth conditions, constructs, and plasmids

The wild-type BW25113 (WT) and the knockout mutant strains of *E. coli* from the KEIO collection used in this study are listed (Table 1). The mutant alleles were freshly introduced into the WT genome by P1 phage transduction. The FLP-recombination and P1 phage transduction methods were employed to generate double and triple mutants (43). The mutant alleles were subjected to PCR amplification and Sanger sequencing to authenticate the genotypes. Δ*RS*::*kan*^{R} and Δ*RS* strains were constructed by deleting the riboswitch region of *mntP* using pKD4 plasmid, RiboS1/S3 oligonucleotides, and λ-red recombination system (43).

The DNA cassettes for the construct 1, 2, 3, and 4 strains were made by fusion PCRs using the appropriate pairs of oligonucleotides from Table S1. The DNA cassettes were cloned into pAH125 or pVenus vectors to get the desired transcriptional fusions (57). The cloned plasmids were then integrated into the genome of the WT strain using pINT helper plasmid and screened for single integrant, as described (57). To generate an *E. coli* strain with *mntP*-FLAG in the chromosome, we employed λ-red recombination system (43), as described in the supplementary materials.

The plasmid pBAD/*Myc*-His A (pBAD) (Invitrogen) was used for *mntP* cloning to generate a pBAD-*mntP* expression vector. PCR products were generated using GK1/GK2 primer pairs and digested with the *HindIII* enzyme. The vectors were digested with *NcoI* enzyme, blunted with Klenow enzyme, and further digested with *HindIII* enzyme. Digested vectors and PCR products were ligated and transformed to generate a pBAD-*mntP* expression vector. Site-directed mutagenesis was

Table 1
The list of strains and plasmids used in this work

Strains and plasmids	Genotype/Features	References
Strains		
BW25113	*Escherichia coli; rrnB3ΔlacZ4787hsdR514Δ(araBAD)* 567 Δ(*rhaBAD*)568 *rph-1*	(58)
Δ*mntP*	BW25113, Δ*mntP::kan*^{R}	(58)
Δ*mntR*	BW25113, Δ*mntR::kan*^{R}	(58)
Δ*mntH*	BW25113, Δ*mntH::kan*^{R}	(58)
Δ*RS::kan*^{R}	BW25113, Δ*RS::kan*^{R}; (*mntP* riboswitch::*kan*^{R})	This study
Δ*RS*	BW25113, Δ*RS::scar*; (*kan*^{R} was removed)	This study
Δ*mntR* Δ*RS*	BW25113, Δ*mntR::kan*^{R}, Δ*RS::scar*	This study
Δ*mntR* Δ*mntH* Δ*RS*	BW25113, Δ*mntR::kan*^{R}, Δ*mntH::kan*^{R}, Δ*RS::scar*	This study
BL21 (DE3)	F− *ompT hsdS*$_B$ (r_B−, m_B−) *gal dcm* (DE3)	Lab collection
C43 (DE3)	A BL21 (DE3) derivative	(59)
Lemo (DE3)	BL21 (DE3) containing the Lemo System	(60)
Plasmids	Features	References
pET28a (+)	*kan*^{R}; T7-promoter; IPTG inducible	Novagen
pET-*mntP*	*mntP* without a stop codon cloned in *NcoI* (blunted) and *HindIII* sites of pET28a (+) vector	This study
pAH125	*kan*^{R}; LacZ reporter	(57)
pVenus	*kan*^{R}; YFP reporter	(57)
pINT	*amp*^{R}; λ-integrase	(57)
pKD4	*amp*^{R}; *kan*^{R} cassette is flanked by FLP recombinase	(43)
pT7A1-*trp t'*	T7A1-trp t' cassette cloned in pGEM-T (Promega)	This study
pBAD/*Myc*-His A	*amp*^{R}; cloning vector	Invitrogen
pBAD-*mntP*	*mntP* cloned in *NcoI* (blunted) and *HindIII* sites of pBAD/*Myc*-His A vector	This study

kan^R, kanamycin resistance; *amp*^{R}, ampicillin resistance.

performed using DD149/DD150 primer pairs to generate pMntP^{D118A} vector from pBAD-*mntP*.

Growth conditions

The bacterial growths were performed in buffered LB broth or media (pH 7.0) at 37 °C. Growth curve analyses were done using a Bioscreen C growth analyzer (Oy Growth Curves Ab Ltd), as described (9). For other assays, the overnight culture of *E. coli* WT cells was diluted 100-fold in the fresh LB medium with or without supplemented 8 mM Mn unless otherwise specified. The cultures were grown for 1.5 h at 37 °C till the O.D.$_{600}$ reached about 0.3. BCM (100 μg/ml) was added at that point and allowed to grow further for 2.5 h at 37 °C. The bacterial pellets were collected, and different assays were performed.

Serial dilution and spot assays

Overnight cultures of the *E. coli* mutants were serially diluted, and 5 μl were spotted on LB-agar plates supplemented with or without 1 mM and 2 mM Mn to visualize the relative sensitivity while growing at 37 °C for 12 h 2 mM Mn nicely resolved the growth differences between the strains (Fig. 4*A*).

RT-PCR analyses

The bacterial cell pellets were collected and quickly washed with 1X PBS. Total RNAs were isolated by TRIzol reagent and a bacterial RNA isolation Kit (Qiagen). DNase I treatment was done. The integrity and quality of the RNA was visualized in a 1% agarose gel. The RNA concentration was determined by a UV-1800 Shimandzu UV-spectrophotometer. 200 ng of RNA samples, primer pairs (Table S1), and GoTaq 1-Step RT-qPCR System (Promega) were used for RT-PCR assays. At least three independent assays were conducted. The change in fold expression in the treated samples was calculated by the $\Delta\Delta C_T$ method using *betB* mRNA RT-PCR as a control.

In vitro transcription assay

The *in vitro* transcription using biotinylated T1 and T2 templates was performed, as described previously (21, 25). Briefly, 20 nM RNA polymerase, 40 nM templates (T1 or T2), 10 μM purified GTP and ATP, 25 μCi of [α-^{32}P] CTP (BRIT), and 10 μM trinucleotide ApUpC (Oligos Etc.) were dissolved in 1X transcription buffer, TB (40 mM Tris-HCl, pH 7.9, 10 mM $MgCl_2$, 50 mM KCl). The reaction mixture was incubated for 5 min at 37 °C to synthesize the initial 13 nucleotide long EC (EC_{13}). 200 μM of nucleotide mixtures (of ATP, GTP, CTP, and UTP) were added to EC_{13} to synthesize RO products, incubating for 10 min at 37 °C. In the Rho-dependent termination assay, 100 nM Rho was added after synthesizing EC_{13} before adding the nucleotide mixtures. The reaction products were mixed with formamide loading dye and heat at 95 °C for 5 min to denature the RNA and other biomolecules. The denatured samples were resolved using a 6% urea-denaturing PAGE.

In another setup, the slurry of streptavidin beads equilibrated with 1X TB was mixed with EC_{13} and incubated for 5 min. Unbound substrates were removed by washing with 1X TB, and reactions were continued with or without Rho. After completion of the reaction, the supernatant portion was separated, and streptavidin beads/pellets were suspended in an equal volume of buffer. Both supernatant and pellet fractions were mixed with formamide loading dye, heated, and ran on a 6% urea-PAGE. The gels were exposed to the phosphor imager screen, and a Typhoon Scanner was used to capture the images.

Western blotting

The western blotting experiments were performed using anti-FLAG polyclonal antibody (Invitrogen). The specificity of the antibody has been confirmed by Western blot experiment using protein extracts from WT cells containing chromosomal

mntP or *mntP*-FLAG ORFs. The *E. coli* WT and ΔRS constructs containing chromosomal *mntP*-FLAG were grown in the absence or presence of Mn for 3 h. The B-PER reagent was used to lyse the cells, and protein contents were estimated by Bradford method. 40 μg of total cellular proteins were loaded on the SDS-PAGE. The proteins were transferred on a nitrocellulose membrane, stained with ponceau S to visualize the loading. Western blotting was done using HRP conjugated goat anti-rabbit secondary antibody and Immobilon Forte western HRP substrate (Millipore).

β-galactosidase assay

For β-galactosidase assays, the bacterial strains (constructs 1, 3, and 4) were grown in the presence or absence of BCM and Mn, as described above. The cell pellets were collected and gently washed twice with Z-buffer (60 mM Na_2HPO_4, 40 mM NaH_2PO_4, 10 mM KCl, and 1 mM $MgSO_4$), and the β-galactosidase assays were performed, as described (9).

YFP reporter fluorescence assay

The overnight cultures were diluted 100-fold in LB broth and grown in the presence or absence of BCM and Mn, as stated above. The cell pellets were collected and washed with 1X phosphate buffer saline (PBS) and then resuspended in 1X PBS. The flow cytometry experiments were performed using a BD FACS accuri instrument for 0.1 million cells using an FL1 laser. The MFI values of three independent experiments with sd were plotted.

Intracellular ROS detection

The overnight primary cultures were diluted 100 folds in LB broth and grown in the presence or absence of 2 mM Mn and 100 μg/ml BCM, as stated above. The cell pellet was washed with 1X PBS and divided into three different fractions, which had approximately equal numbers of cells. Of the three, one fraction was stained by 2 μM DHE, the other by 10 μM H_2DCFDA for 1 hour, and the third fraction was dissolved in 1X PBS. The data was acquired using FACS accuri (BD) at FL1 laser for H_2DCFDA and FL2 laser for DHE for 0.05 million cells. Mean fluorescence intensity (MFI) values obtained from three different experiments were plotted after deducting the background fluorescence values.

Confocal microscopy analyses

The cell morphologies and filamentations were visualized using an in-house confocal Nikon confocal microscope. The overnight cultures of the WT and ΔRS *E. coli* strains were diluted 100-fold in fresh LB broth and were grown for 1.5 h at 37 °C till the $O.D._{600}$ reached about 0.3. The cultures were further grown in the presence or absence of 2 mM $MnCl_2$ for 2.5 h (for Fig. 4*C*). In case of Figure 6*B*, the arabinose was added from the beginning till 4 h of growth. The cell pellets were collected and washed with PBS. The cells were fixed with 4% formaldehyde and examined. The images were captured, and the relative cell lengths (50 cells for each condition) were measured by Image J. software. The mean and sd values were calculated.

ICP MS analyses

The overnight culture of the WT and ΔRS strains was diluted 100-fold in fresh LB broth and was grown for 1.5 h at 37 °C till the $O.D._{600}$ reached about 0.3. The WT culture was further grown in the presence or absence of 100 μg/ml of BCM for 2.5 h (for Fig. 3*C*). In the case of the ΔRS strain, the growth was continued for another 2.5 h in the presence or absence of 2 mM $MnCl_2$ (for Fig. 5*E*). The cell pellets were collected, and ICP-MS analyses were done, as described (9).

Data availability

All manuscript data are available in the manuscript files.

Supporting information—This article contains Supporting information (43).

Acknowledgments—The authors are grateful to Dr Rachna Chaba lab, IISER Mohali, India for generously providing some plasmid and strains listed in Table 1. Dr Debabrata Mondal and Shivanand, the DD lab members, assisted to perform some revised experiments. A.*P. and* A.K. are DBT fellow and DST-Inspire fellow, respectively. R.K.M. and N.V. are UGC fellows. K.B. and D.G. are CSIR fellows. BP is Senior Research Scientist, NYUMC. EN is Julie Wilson Anderson Professor, and HHMI fellow.

Author contributions—A. K., K. B., and A. P. writing–original draft; A. K., K. B., and A. P. visualization; A. K., K. B., A. P., D. D., B. P., G. K., N. V., R. K. M., and D. G. validation; A. K., K. B., A. P., D. D., B. P., G. K., N. V., R. K. M., and D. G. methodology; A. K., K. B., A. P., G. K., N. V., R. K. M., and D. G. investigation; A. K., K. B., A. P., D. D., B. P., R. K. M., and D. G. formal analysis; A. P., D. D., and B. P. writing–review & editing, D. D. supervision; D. D. resources; D. D. funding acquisition.

Funding and additional information—This work received financial support from intramural grants of CSIR, India (MLP-0042) and CSIR-IMTECH, India (OLP-0190), and by an extramural grant to D.D. from SERB, India (CRG/2019/001174), Department of Science and Technology (DST).

Conflict of interest—The authors declare that they have no conflicts of interest with the contents of this article.

Abbreviations—The abbreviations used are: BCM, bicyclomycin; EC, elongation complex; MFI, mean fluorescence intensity; Mn, manganese; ORF, open reading frame; RO, run-off; ROS, reactive oxygen species; UTR, untranslated region.

References

1. Imlay, J. A. (2014) The mismetallation of enzymes during oxidative stress. *J. Biol. Chem.* **289**, 28121–28128
2. Ikeda, J. S., Janakiraman, A., Kehres, D. G., Maguire, M. E., and Slauch, J. M. (2005) Transcriptional regulation of sitABCD of Salmonella enterica serovar Typhimurium by MntR and Fur. *J. Bacteriol.* **187**, 912–922

3. Kehres, D. G., Janakiraman, A., Slauch, J. M., and Maguire, M. E. (2002) Regulation of Salmonella enterica serovar Typhimurium mntH transcription by H(2)O(2), Fe(2+), and Mn(2+). *J. Bacteriol.* **184**, 3151–3158
4. Anjem, A., and Imlay, J. A. (2012) Mononuclear iron enzymes are primary targets of hydrogen peroxide stress. *J. Biol. Chem.* **287**, 15544–15556
5. Sobota, J. M., and Imlay, J. A. (2011) Iron enzyme ribulose-5-phosphate 3-epimerase in Escherichia coli is rapidly damaged by hydrogen peroxide but can be protected by manganese. *Proc. Natl. Acad. Sci. U. S. A.* **108**, 5402–5407
6. Waters, L. S., Sandoval, M., and Storz, G. (2011) The Escherichia coli MntR miniregulon includes genes encoding a small protein and an efflux pump required for manganese homeostasis. *J. Bacteriol.* **193**, 5887–5897
7. Kaur, G., Kumar, V., Arora, A., Tomar, A., Ashish, Sur, R., *et al.* (2017) Affected energy metabolism under manganese stress governs cellular toxicity. *Sci. Rep.* **7**, 11645
8. Martin, J. E., Waters, L. S., Storz, G., and Imlay, J. A. (2015) The Escherichia coli small protein MntS and exporter MntP optimize the intracellular concentration of manganese. *PLoS Genet.* **11**, e1004977
9. Kalita, A., Mishra, R. K., Kumar, V., Arora, A., and Dutta, D. (2022) An intrinsic alkalization circuit turns on mntP riboswitch under manganese stress in Escherichia coli. *Microbiol. Spectr.* **10**, e0336822
10. Dambach, M., Sandoval, M., Updegrove, T. B., Anantharaman, V., Aravind, L., Waters, L. S., *et al.* (2015) The ubiquitous yybP-ykoY riboswitch is a manganese-responsive regulatory element. *Mol. Cell* **57**, 1099–1109
11. Serganov, A., and Nudler, E. (2013) A decade of riboswitches. *Cell* **152**, 17–24
12. Serganov, A., and Patel, D. J. (2012) Molecular recognition and function of riboswitches. *Curr. Opin. Struct. Biol.* **22**, 279–286
13. Henkin, T. M. (2008) Riboswitch RNAs: using RNA to sense cellular metabolism. *Genes Dev.* **22**, 3383–3390
14. Price, I. R., Gaballa, A., Ding, F., Helmann, J. D., and Ke, A. (2015) Mn(2+)-sensing mechanisms of yybP-ykoY orphan riboswitches. *Mol. Cell* **57**, 1110–1123
15. Barrick, J. E., Corbino, K. A., Winkler, W. C., Nahvi, A., Mandal, M., Collins, J., *et al.* (2004) New RNA motifs suggest an expanded scope for riboswitches in bacterial genetic control. *Proc. Natl. Acad. Sci. U. S. A.* **101**, 6421–6426
16. Meyer, M. M., Hammond, M. C., Salinas, Y., Roth, A., Sudarsan, N., and Breaker, R. R. (2011) Challenges of ligand identification for riboswitch candidates. *RNA Biol.* **8**, 5–10
17. Sun, E. I., Leyn, S. A., Kazanov, M. D., Saier, M. H., Jr., Novichkov, P. S., and Rodionov, D. A. (2013) Comparative genomics of metabolic capacities of regulons controlled by cis-regulatory RNA motifs in bacteria. *BMC Genomics* **14**, 597
18. Helmann, J. D. (2014) Specificity of metal sensing: iron and manganese homeostasis in Bacillus subtilis. *J. Biol. Chem.* **289**, 28112–28120
19. Oh, Y. K., and Freese, E. (1976) Manganese requirement of phosphoglycerate phosphomutase and its consequences for growth and sporulation of Bacillus subtilis. *J. Bacteriol.* **127**, 739–746
20. Que, Q., and Helmann, J. D. (2000) Manganese homeostasis in Bacillus subtilis is regulated by MntR, a bifunctional regulator related to the diphtheria toxin repressor family of proteins. *Mol. Microbiol.* **35**, 1454–1468
21. Huang, X., Shin, J. H., Pinochet-Barros, A., Su, T. T., and Helmann, J. D. (2017) Bacillus subtilis MntR coordinates the transcriptional regulation of manganese uptake and efflux systems. *Mol. Microbiol.* **103**, 253–268
22. Nudler, E., and Gottesman, M. E. (2002) Transcription termination and anti-termination in E. coli. *Genes Cells* **7**, 755–768
23. Richardson, J. P. (2002) Rho-dependent termination and ATPases in transcript termination. *Biochim. Biophys. Acta* **1577**, 251–260
24. Dutta, D., Chalissery, J., and Sen, R. (2008) Transcription termination factor rho prefers catalytically active elongation complexes for releasing RNA. *J. Biol. Chem.* **283**, 20243–20251
25. Boudvillain, M., Nollmann, M., and Margeat, E. (2010) Keeping up to speed with the transcription termination factor Rho motor. *Transcription* **1**, 70–75
26. Mooney, R. A., Davis, S. E., Peters, J. M., Rowland, J. L., Ansari, A. Z., and Landick, R. (2009) Regulator trafficking on bacterial transcription units in vivo. *Mol. Cell* **33**, 97–108
27. Peters, J. M., Vangeloff, A. D., and Landick, R. (2011) Bacterial transcription terminators: the RNA 3′-end chronicles. *J. Mol. Biol.* **412**, 793–813
28. Epshtein, V., Dutta, D., Wade, J., and Nudler, E. (2010) An allosteric mechanism of Rho-dependent transcription termination. *Nature* **463**, 245–249
29. Sullivan, S. L., and Gottesman, M. E. (1992) Requirement for E. coli NusG protein in factor-dependent transcription termination. *Cell* **68**, 989–994
30. Burns, C. M., Nowatzke, W. L., and Richardson, J. P. (1999) Activation of Rho-dependent transcription termination by NusG. Dependence on terminator location and acceleration of RNA release. *J. Biol. Chem.* **274**, 5245–5251
31. Cardinale, C. J., Washburn, R. S., Tadigotla, V. R., Brown, L. M., Gottesman, M. E., and Nudler, E. (2008) Termination factor Rho and its cofactors NusA and NusG silence foreign DNA in E. coli. *Science* **320**, 935–938
32. Ciampi, M. S. (2006) Rho-dependent terminators and transcription termination. *Microbiology (Reading)* **152**, 2515–2528
33. Rabhi, M., Tuma, R., and Boudvillain, M. (2010) RNA remodeling by hexameric RNA helicases. *RNA Biol.* **7**, 655–666
34. Mitra, P., Ghosh, G., Hafeezunnisa, M., and Sen, R. (2017) Rho protein: roles and mechanisms. *Annu. Rev. Microbiol.* **71**, 687–709
35. Hollands, K., Proshkin, S., Sklyarova, S., Epshtein, V., Mironov, A., Nudler, E., *et al.* (2012) Riboswitch control of Rho-dependent transcription termination. *Proc. Natl. Acad. Sci. U. S. A.* **109**, 5376–5381
36. Hollands, K., Sevostiyanova, A., and Groisman, E. A. (2014) Unusually long-lived pause required for regulation of a Rho-dependent transcription terminator. *Proc. Natl. Acad. Sci. U. S. A.* **111**, E1999–E2007
37. Pedrolli, D., Langer, S., Hobl, B., Schwarz, J., Hashimoto, M., and Mack, M. (2015) The ribB FMN riboswitch from Escherichia coli operates at the transcriptional and translational level and regulates riboflavin biosynthesis. *FEBS J.* **282**, 3230–3242
38. Takemoto, N., Tanaka, Y., and Inui, M. (2015) Rho and RNase play a central role in FMN riboswitch regulation in Corynebacterium glutamicum. *Nucleic Acids Res.* **43**, 520–529
39. Bastet, L., Chauvier, A., Singh, N., Lussier, A., Lamontagne, A. M., Prevost, K., *et al.* (2017) Translational control and Rho-dependent transcription termination are intimately linked in riboswitch regulation. *Nucleic Acids Res.* **45**, 7474–7486
40. Zwiefka, A., Kohn, H., and Widger, W. R. (1993) Transcription termination factor rho: the site of bicyclomycin inhibition in Escherichia coli. *Biochemistry* **32**, 3564–3570
41. Richardson, L. V., and Richardson, J. P. (1996) Rho-dependent termination of transcription is governed primarily by the upstream Rho utilization (rut) sequences of a terminator. *J. Biol. Chem.* **271**, 21597–21603
42. Wu, A. M., Christie, G. E., and Platt, T. (1981) Tandem termination sites in the tryptophan operon of Escherichia coli. *Proc. Natl. Acad. Sci. U. S. A.* **78**, 2913–2917
43. Datsenko, K. A., and Wanner, B. L. (2000) One-step inactivation of chromosomal genes in Escherichia coli K-12 using PCR products. *Proc. Natl. Acad. Sci. U. S. A.* **97**, 6640–6645
44. Zeinert, R., Martinez, E., Schmitz, J., Senn, K., Usman, B., Anantharaman, V., *et al.* (2018) Structure-function analysis of manganese exporter proteins across bacteria. *J. Biol. Chem.* **293**, 5715–5730
45. Platt, T. (1986) Transcription termination and the regulation of gene expression. *Annu. Rev. Biochem.* **55**, 339–372
46. Proshkin, S., Rahmouni, A. R., Mironov, A., and Nudler, E. (2010) Cooperation between translating ribosomes and RNA polymerase in transcription elongation. *Science* **328**, 504–508
47. Breaker, R. R. (2012) Riboswitches and the RNA world. *Cold Spring Harb Perspect. Biol.* **4**, a003566
48. Barrick, J. E., and Breaker, R. R. (2007) The distributions, mechanisms, and structures of metabolite-binding riboswitches. *Genome Biol.* **8**, R239

49. Miwa, Y., Horiguchi, T., and Shigesada, K. (1995) Structural and functional dissections of transcription termination factor rho by random mutagenesis. *J. Mol. Biol.* **254**, 815–837
50. Ingham, C. J., Dennis, J., and Furneaux, P. A. (1999) Autogenous regulation of transcription termination factor Rho and the requirement for Nus factors in Bacillus subtilis. *Mol. Microbiol.* **31**, 651–663
51. Quirk, P. G., Dunkley, E. A., Jr., Lee, P., and Krulwich, T. A. (1993) Identification of a putative Bacillus subtilis rho gene. *J. Bacteriol.* **175**, 647–654
52. Drew, D., Froderberg, L., Baars, L., and de Gier, J. W. (2003) Assembly and overexpression of membrane proteins in Escherichia coli. *Biochim. Biophys. Acta* **1610**, 3–10
53. Wagner, S., Baars, L., Ytterberg, A. J., Klussmeier, A., Wagner, C. S., Nord, O., *et al.* (2007) Consequences of membrane protein overexpression in Escherichia coli. *Mol. Cell Proteomics* **6**, 1527–1550
54. Wagner, S., Klepsch, M. M., Schlegel, S., Appel, A., Draheim, R., Tarry, M., *et al.* (2008) Tuning Escherichia coli for membrane protein overexpression. *Proc. Natl. Acad. Sci. U. S. A.* **105**, 14371–14376
55. Gubellini, F., Verdon, G., Karpowich, N. K., Luff, J. D., Boel, G., Gauthier, N., *et al.* (2011) Physiological response to membrane protein overexpression in E. coli. *Mol. Cell Proteomics* **10**, M111.007930
56. Singh, G. P., and Dash, D. (2013) Electrostatic mis-interactions cause overexpression toxicity of proteins in E. coli. *PLoS One* **8**, e64893
57. Haldimann, A., and Wanner, B. L. (2001) Conditional-replication, integration, excision, and retrieval plasmid-host systems for gene structure-function studies of bacteria. *J. Bacteriol.* **183**, 6384–6393
58. Baba, T., Ara, T., Hasegawa, M., Takai, Y., Okumura, Y., Baba, M., *et al.* (2006) Construction of Escherichia coli K-12 in-frame, single-gene knockout mutants: the Keio collection. *Mol. Syst. Biol.* **2**, 2006.0008
59. Miroux, B., and Walker, J. E. (1996) Over-production of proteins in Escherichia coli: mutant hosts that allow synthesis of some membrane proteins and globular proteins at high levels. *J. Mol. Biol.* **260**, 289–298
60. Schlegel, S., Lofblom, J., Lee, C., Hjelm, A., Klepsch, M., Strous, M., *et al.* (2012) Optimizing membrane protein overexpression in the Escherichia coli strain Lemo21(DE3). *J. Mol. Biol.* **423**, 648–659